High phosphate content significantly increases apatite formation of fluoride-containing bioactive glasses

Mohammed Mneimne[a], Robert G. Hill[a], Andrew J. Bushby[b], Delia S. Brauer[*,a]

[a]Unit of Dental Physical Sciences, Barts and The London, Mile End Road, London E1 4NS, UK

[b]Department of Materials, Queen Mary University of London, Mile End Road, London E1 4NS, UK

*Corresponding author. Tel.: +44 (0)207 882 5964; fax: +44 (0)207 882 7979. *E-mail address*: d.brauer@qmul.ac.uk.

Abstract

Bioactive glass-containing toothpastes for treating dentine hypersensitivity work by precipitating hydroxy-carbonate apatite (HCA) onto the tooth surface, but concerns exist over the long-term durability of HCA in the mouth. Fluoride-containing bioactive glasses form fluorapatite (FAp) in physiological solutions, which is more chemically stable against acid attack.

The influence of phosphate content on apatite formation was investigated by producing a low-phosphate (about 1 mol% P_2O_5) and a high-phosphate (about 6 mol%) series of melt-derived bioactive glasses in the system SiO_2-P_2O_5-CaO-Na_2O; increasing amounts of CaF_2 were added by keeping the ratio of all other components constant. pH change, ion release and apatite formation during immersion in tris buffer at 37°C over up to seven days were investigated. Crystal phases formed in tris buffer were characterised using infra-red spectroscopy, X-ray diffraction and solid-state nuclear magnetic resonance.

An increase in phosphate or fluoride content allowed for apatite formation at lower pH; fluoride enhanced apatite formation due to lower solubility of FAp compared to hydroxyapatite or HCA. High phosphate content glasses formed apatite significantly faster (within 6 hours) than low phosphate content glasses (within 3 days). In addition, an increase in phosphate content favoured apatite formation rather than fluorite (CaF_2). ^{19}F MAS NMR showed the apatite formed by fluoride-containing glasses to be FAp, which makes these glasses of particular interest for dental applications. This study shows that by varying the phosphate content the reactivity and apatite formation of bioactive glasses can be controlled successfully.

Key words

dentifrices; toothpaste; fluoride; bioactive glass; fluorapatite; apatite

Introduction

Bioactive glasses are known to undergo surface reactions and form a layer of hydroxy-carbonated apatite (HCA) on the surface when exposed to body fluids. These glasses have been extensively studied in the literature and have found use as bone substitute materials as they promote bone formation and osseointegration [1]. More recently these glasses have found application in dentistry as a remineralising additive for toothpastes, particularly for treating dentine hypersensitivity [2,3]. Dentine hypersensitivity is caused by dentinal tubules of root dentine being exposed, and the toothpaste contains bioactive glass with a large fraction of particles small enough (< 3 μm) to enter the dentinal tubules. Formation of apatite then occludes the tubules and thus reduces sensitivity. Formation of fluorapatite (FAp) rather than HCA is preferable, as it is more chemically stable at lower pH and would therefore less readily dissolve when the mouth is exposed to acidic conditions (*e.g.* during consumption of fruit juice and carbonated beverages). We have recently showed that fluoride-containing bioactive glasses form FAp in SBF [4]. However, the glass component of the toothpaste needs to perform its function and form FAp before it is diluted away by salivary action. Ideally, it should form FAp in the mouth in less than 8 hours, corresponding to an overnight period where salivary flow will be minimal. It must also not raise the pH significantly above 7.4 when used at high loadings (up to 10% by weight) in the toothpaste.

Fluorides have been added to non-fluorine bioactive glass containing toothpastes; however, here the more soluble fluoride salt is likely to give a high fluoride concentration before the calcium concentration is increased by dissolution of the glass and is likely to result in fluorite (CaF_2) formation, which may inhibit subsequent FAp formation. It is better to deliver Ca^{2+}, PO_4^{3-} and F^- ions together in the appropriate amounts to form FAp from a single glass composition in order to avoid the possible formation of CaF_2.

In bioactive glasses phosphate is present as orthophosphate as shown by ^{31}P and ^{29}Si MAS NMR [5,6]. We hypothesised that an increase in P_2O_5 content (while adding additional Na_2O and CaO to maintain a fixed network connectivity, NC [7]) in fluoride-containing glasses would result in an increase in glass degradation and ion release and would favour formation of FAp rather than fluorite. We produced two series of glasses in the system SiO_2–P_2O_5–CaO–Na_2O, one with a low phosphate content (about 1 mol% P_2O_5) and another one with a high phosphate content (about 6 mol%) with increasing concentrations of CaF_2. NC was fixed by adding CaF_2 (rather than substituting for CaO) while the ratio of all other components was kept constant, assuming that fluoride stays associated with calcium, *i.e.* no Si-F bonds are formed [8,9]. We performed degradation experiments in tris buffer to demonstrate the effects of glass composition on degradation, pH and *in vitro* apatite formation of fluoride-containing bioactive glasses.

Materials and methods

Glass synthesis

Glasses in the system SiO_2–P_2O_5–CaO–Na_2O were prepared using a melt–quench route. A series with low (about 1 mol% P_2O_5) and one with high (about 6 mol% P_2O_5) were produced. CaF_2 was added in increasing amounts while network connectivity (NC) and the ratio of all other components were kept constant (glasses A to F and A2 to F2, Tables 1 and 2). In addition, one sodium-free glass was synthesised for each glass series (glasses H and H2, Tables 1 and 2). Glasses in the high phosphate content series were produced by increasing the phosphate content, whilst adding additional Na_2O and CaO in order to maintain a fixed NC.

Table 1:   Nominal glass composition of the low phosphate content glasses in mol%; theoretical network connectivity (NC) is 2.13.

Glass	SiO_2	P_2O_5	CaO	Na_2O	CaF_2
A	49.47	1.07	23.08	26.38	-
B	47.12	1.02	21.98	25.13	4.75
C	44.88	0.97	20.94	23.93	9.28
D	42.73	0.92	19.94	22.79	13.62
E	40.68	0.88	18.98	21.69	17.76
F	36.83	0.80	17.18	19.64	25.54
H	44.88	0.97	44.87	-	9.28

Mixtures of analytical grade SiO_2 (Prince Minerals Ltd., Stoke-on-Trent, UK), P_2O_5, $CaCO_3$, Na_2CO_3 and CaF_2 (all Sigma-Aldrich, Gillingham, UK) were melted in a platinum-rhodium crucible for 1 h at 1430°C in an electric furnace (EHF 17/3, Lenton, Hope Valley, UK). A batch size of approximately 100 g was used. After melting, the glasses were rapidly quenched into water to prevent crystallisation. After drying, the glass was ground using a vibratory mill (Gyro mill, Glen Creston, London, UK) for 7 min and sieved using a 38 µm mesh analytical sieve (Endecotts Ltd., London, UK). The amorphous structure of the glasses was confirmed by powder X-ray diffraction (XRD; X'Pert PRO MPD, PANalytical, Cambridge, UK; 40 kV/40 mA, CuKα, data collected at room temperature).

Table 2:   Nominal glass composition of the high phosphate content glasses in mol%; theoretical network connectivity (NC) is 2.08.

Glass	SiO_2	P_2O_5	CaO	Na_2O	CaF_2
A2	38.14	6.33	25.91	29.62	-
B2	36.41	6.04	24.74	28.28	4.53
C2	34.60	5.74	23.51	26.87	9.28
D2	32.95	5.47	22.38	25.59	13.62
E2	31.37	5.21	21.31	24.36	17.76
F2	28.40	4.71	19.29	22.06	25.54
H2	34.60	5.74	50.38	-	9.28

pH and ion release in tris buffer

Tris buffer solution was prepared by dissolving 15.090 g tris(hydroxymethyl)aminomethane (Sigma-Aldrich) in ca. 800 mL deionised water, adding 44.2 mL 1 M hydrochloric acid (Sigma-Aldrich), heating to 37°C over night, adjusting the pH to 7.30 using 1 M hydrochloric acid using a pH meter (Oakton Instruments, Nijkerk, Netherlands) and filling to a total volume of 2000 mL using deionised water. Tris buffer solution was kept at 37°C.

50 mL tris buffer were pipetted into 150 mL PE bottles. pH was measured using a pH meter (Oakton Instruments) and 75 mg of glass powder (< 38 μm) were dispersed in the tris buffer solution, corresponding to a concentration of 1.5 g/L. Experiments were performed in duplicate. Samples were placed in an orbital shaker at 37°C at an agitation rate of 60 Hz for up to 1 week. Tris buffer from the same batch without glass powder was used as control. pH was measured at 1, 3, 7 and 14 days.

After removing the samples from the shaker pH was measured and solutions were filtered through medium porosity filter paper (5 μm particle retention, VWR International, Lutterworth, UK) and kept at 4°C.

Fluoride-release into tris buffer was measured using a fluoride-selective electrode (Orion 9609BNWP with Orion pH/ISE meter 710, both Thermo Scientific, Waltham, MA, USA). Calibration was performed using standard solutions prepared using tris buffer to account for ionic strength.

Undiluted solutions (for analysis of phosphorus) as well as samples diluted by a factor 1:5 (for analysis of silicon, sodium and calcium) were acidified using 69% nitric acid and quantitatively analysed by inductively coupled plasma – optical emission spectroscopy (ICP; Varian Vista-PRO, Varian Ltd., Oxford, UK).

Characterisation of glass powders after immersion in tris buffer

Filter paper was dried at 37°C and the dried powders were analysed using Fourier-transform infrared spectroscopy (FTIR; Spectrum GX, Perkin-Elmer, Waltham, MA, USA; data collected from 1600 to 500 cm^{-1}) and XRD (X'Pert PRO MPD, PANalytical, Cambridge, UK; 40 kV/40 mA, CuKα, data collected at room temperature with a 0.033°2θ step size and a count rate of 99.6 s per step, from 2θ values of 10° to 60°).

^{19}F magic angle spinning nuclear magnetic resonance (MAS NMR) experiments on tris-treated glass powders were performed using a Bruker 200 MHz (4.7 T) spectrometer. ^{19}F NMR data were collected at a Larmor frequency of 188.2 MHz under spinning conditions of 12.5 kHz in a 4 mm rotor. A low fluorine content probe was used, making background subtraction unnecessary. ^{19}F chemical shift scale was referenced using the -120 ppm peak of 1 M NaF aqueous solution as a secondary reference against CFCl$_3$.

Results and Discussion

Glass formation

Low phosphate content glasses were obtained in an amorphous state as shown earlier [8]. The XRD patterns of milled high phosphate content glasses A2 to F2 (see Supplementary Figure S1) show the typical amorphous halo, indicating the glassy state of the material. There is evidence of very small amounts of apatite in the sodium free glass (H2) as shown by the two peaks at 32 and 33°2θ, and crystallisation of small amounts of apatite is likely to have occurred during quenching.

[19]F magic angle spinning nuclear magnetic resonance spectroscopy (MAS NMR) showed previously [8] that by adding CaF_2 to the composition (and keeping the ratio of all other components constant) rather than substituting it for CaO the network connectivity [10] of the glass and the *Q* speciation (*i.e.* the number of bridging and non-bridging oxygens per silicate structural unit) remained unchanged. This contrasts with the previous studies on fluoride-containing bioactive glasses [11,12] where CaF_2 was substituted for CaO, which resulted in a more cross-linked glass and greatly reduced dissolution rate and bioactivity.

Effect of fluoride content on pH of tris buffer

Soda-lime phosphosilicate-based bioactive glasses (such as Bioglass[®] 45S5) are well known to cause a pH rise upon immersion in aqueous solutions [13]. This pH increase favours apatite deposition but can negatively affect the surrounding tissue *in vivo*, a problem which is largely overlooked in the literature. Too high a pH rise is also a disadvantage for toothpaste applications, as it could negatively affect the oral mucosa.

The fluoride-releasing glasses in this work clearly showed a pH rise within the first 24 hours of immersion in tris buffer; shown in Figure 1. The low phosphate content glasses were previously shown to give a similar pH rise in SBF [4]; however, due to a higher buffering capacity of the tris buffer solution compared to SBF the pH rise is less pronounced in the current study. Low phosphate glasses show a further increase in pH (Figure 1a) between 24 hours and 3 days; the pH decrease at day 7 can be explained by a lower initial pH of the tris buffer solution (7.31 compared to 7.34). By comparison, high phosphate content glasses (Figure 1b) reach their maximum pH within the first 24 hours; after this initial pH rise the pH stayed constant over the remaining time of the experiment.
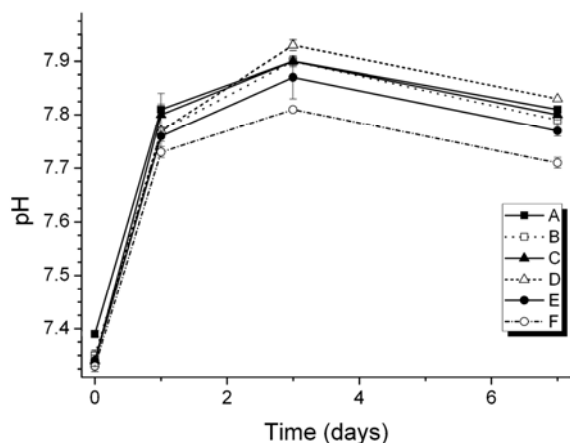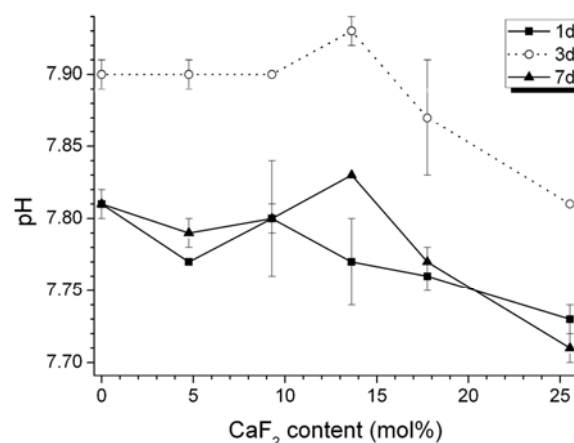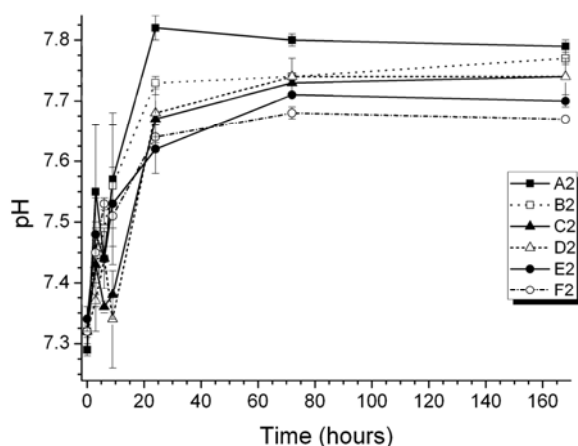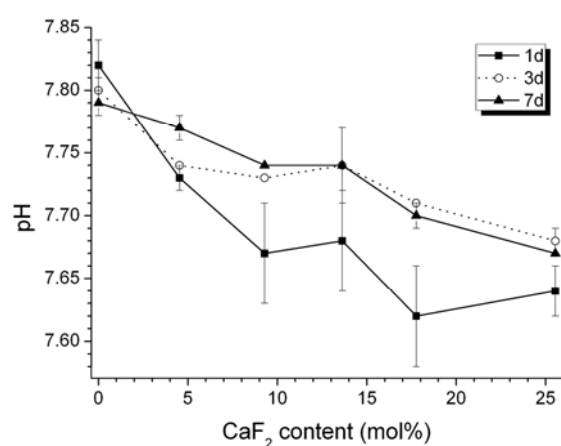
Figure 1: pH of tris buffer solution after immersion of (a) low phosphate and (b) high phosphate glasses *vs.* time and (c) low and (d) high phosphate content glass powder *vs.* CaF$_2$ content in the glass. (Lines are drawn as a guide to the eye.)

The pH rise is less pronounced for high phosphate content glasses compared to low phosphate content glasses; pH values of high phosphate content glasses are between 0.04 and 0.2 lower than the corresponding values for the low phosphate content glasses. Details are shown for glasses A to F and A2 to F2 at 3 days as well as for the two sodium-free compositions (H and H2) over time in Supplementary Figure S2. pH values found for sodium-free glasses H and H2 are comparable to those found for glasses C and C2, which are the corresponding sodium-containing glasses. O'Donnell *et al.* [14] explained the effect of phosphate content on the pH by the release of more phosphate from the glass, which buffers the alkalinity caused by sodium and calcium ions.

The pH rise was also less pronounced for increasing fluoride contents in the glass (Figures 1c, d), both in the low and high phosphate series: There is a small but significant reduction in pH with increasing fluorine content of the glass which mirrors that found for the low phosphate content glasses in SBF [4]. The effect of fluoride content in the glass on the pH in aqueous solution can be explained by ion exchange processes on the glass surface: cations such as Na$^+$ or Ca^{2+}

near the glass surface can go into solution in exchange for H^+ ions from the solution (from dissociation of water into H^+ and OH^-), which results in a pH increase. Similarly, F^- ions can be exchanged for OH^- ions, thereby removing hydroxyl ions from solution; therefore for increasing fluoride content in the glass the pH rise is less pronounced.

The resulting pH depends on the particle size/surface area and the concentration of the glass as well as on the buffering capacity of the surrounding solution, and although the pH values shown here are ≤ 7.9 under the experimental conditions in this research, pH values in the oral cavity might potentially be higher depending on the loading of glass in the toothpaste and the amount of saliva present. Our results clearly show the potential of increased phosphate and fluoride contents on controlling the pH upon glass degradation.

Apatite deposition in tris buffer

Conventionally the "bioactivity" (defined as apatite formation) of bioactive glasses is assessed by immersing the glass in simulated body fluid (SBF), which is a solution saturated in calcium and phosphate, and which mimics the ionic concentrations found in blood plasma [15]. If the glass results in the formation of apatite in the designated time period it is conventionally termed bioactive. However, the saliva in the mouth is diluted after taking in liquids and often no longer saturated with regard to Ca^{2+} and PO_4^{3-}. For this reason we have investigated the apatite forming ability of the glasses in tris buffer containing no Ca^{2+} and PO_4^{3-}, as this represents a more severe test of bioactivity. Formation of apatite was followed using FTIR, XRD and ^{19}F solid-state MAS NMR.

FTIR spectra of all glass compositions showed significant changes after immersion in tris buffer in comparison to the spectrum of the unreacted glass (shown in Figures 2a, b for glasses B and B2, respectively). The bands for the untreated glass powder were mostly due to Si-O vibrational modes: Si-O stretch, Si-O alkali stretch and Si-O bend [16], which will be described in the following. After immersion in tris buffer all spectra showed the following changes: disappearance of the non-bridging oxygen (NBO, Si-O$^-$ alkali$^+$) band at 920 cm^{-1} and sharpening of the Si-O-Si stretch band at about 1030 cm^{-1}. At the same time, new bands appeared at about 790 cm^{-1}, which were assigned to Si-O-Si bond vibration between two adjacent SiO_4 tetrahedra as described previously for SBF-treated glasses [4]. These changes indicate formation of a silica-gel surface layer after leaching of Ca^{2+} and Na^+ ions and formation of Si-OH groups in this ion depleted glass. Spectra after tris buffer immersion for 1 week (Figures 3a, b) showed either a single band or a split band at approximately 560 cm^{-1}. This is the most characteristic region for apatite and other phosphates, and it corresponds to P-O bonding vibrations in a PO_4^{3-} tetrahedron and indicates presence of crystalline calcium phosphates including hydroxyapatite (HAp) and HCA [16]. A single band in this region suggests presence of non-apatitic or amorphous calcium phosphate (ACP) which is usually taken as indication of presence of precursors to apatite [17]. Apatitic PO_4^{3-} groups give characteristic split bands at 560 and 600 cm^{-1} [18], with a third signal at 575 cm^{-1} [19]

observed for crystallites of small size. Both glass B and glass B2 (Figures 2a, b) show clear presence of a split band in this range at 3 days (glass B) and 6 hours (glass B2) which suggests that an increase in phosphate content (from 1.02 mol% in glass B to 6.04 mol% in glass B2) resulted in significantly faster apatite formation. For all glasses showing a split band (Figures 3a, b), a shoulder is present at 575 cm^{-1} indicating the small size of the calcium phosphate crystallites. This is confirmed by crystallite size analysis of apatite formed on bioactive glasses in SBF by O'Donnell *et al.* [14], which showed crystal sizes in the range of 16 to 26 nm, and crystallites in our study are also likely to be in the nanometer size range (below 50 nm).
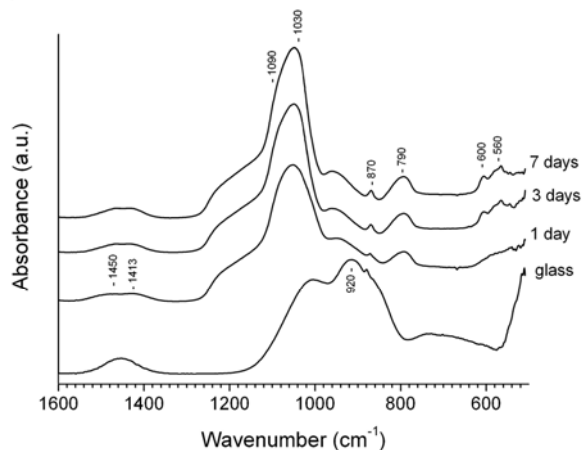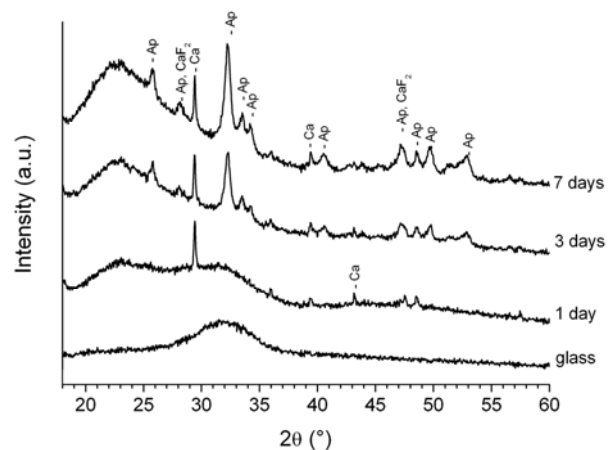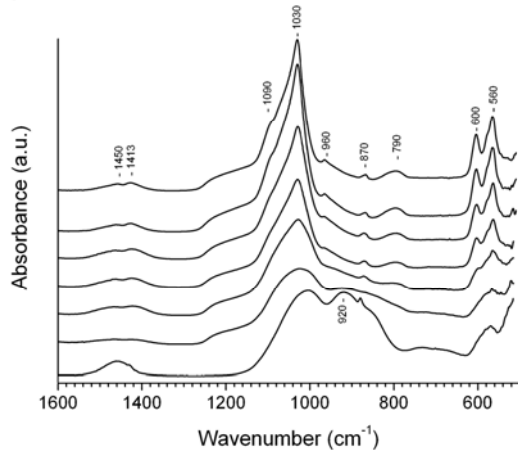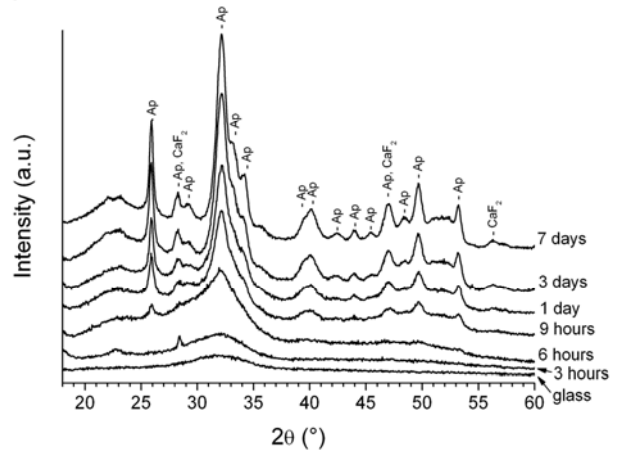
Figure 2: FTIR spectra (a, b) and XRD patterns (c, d) of glasses B (top, low phosphate) and B2 (bottom, high phosphate) before ("glass") and after immersion in tris buffer at different time points.

Presence of carbonate substitution in the apatite is indicated by the band at about 870 cm^{-1} present in all glasses at 1 week immersion in tris buffer (Figures 3a, b). In SBF treated glass, this carbonate band is usually taken as an indication for carbonate being incorporated into the apatite, resulting in HCA rather than stoichiometric HAp [20]. It is difficult to distinguish whether this band is split, in which case it would be B-type substitution (*i.e.* carbonate replacing a phosphate group). However, for most of the compositions treated in tris buffer for 1 week (Figures 3a, b) broad CO_3^{2-} bands are

present in the region starting from 1410 cm^{-1} which indicates B-type substitution. The CO_3^{2-} signal for A-type substitution (*i.e.* carbonate replacing a hydroxyl group) would be shifted to higher wavenumbers, starting from 1460 cm^{-1}. Spectra also showed a shoulder at 1080 to 1090 cm^{-1} which corresponds to a P-O stretch which is also observed in B-type substituted HCA [18]. At 1 week, it is most clearly pronounced in the high phosphate content glasses (Figure 3b) which is consistent with the more clearly pronounced split apatitic bands at 560 and 600 cm^{-1}.

Figures 2c, d show XRD patterns of glasses B and B2 before (*i.e.* untreated glass) and at various time points of immersion in tris buffer. All experimental XRD patterns were compared to reference patterns of hydroxyapatite (JCPDS 09-432), fluorapatite (15-876), hydroxy-carbonate apatite (JCPD 19-272) and carbonated fluorapatite (JCPDS 31-267); however, as these patterns overlap we will refer to the pattern of HAp in the following, although phases formed for glasses in the low phosphate content series in SBF were identified to be fluorapatite by ^{19}F MAS NMR [4].

At 1 day, glass B (Figure 2c) shows presence of calcite peaks only (calcium carbonate, JCPD 5-586); at 3 days the typical apatite peaks at 26 and 32 to 34°2θ appear, superimposed on an amorphous halo. At 1 week, these peaks become larger in intensity and more clearly pronounced. For glass B2 (Figure 2d) the XRD pattern at 3 hours of tris immersion shows a small peak appearing at 28.5°2θ, which might suggest presence of apatite. However, due to the absence of other characteristic peaks, assigning this peak to a crystal phase is difficult. At 6 hours, however, a small peak appears at 26°2θ and a broad peak between 32 and 34°2θ, all of which are superimposed on an amorphous halo and which clearly indicate presence of apatite. The low peak intensity suggests that the amount of apatite is small, while the line broadening (and the resulting broad feature between 32 and 34°2θ rather than clearly resolved individual peaks) is due to a small crystallite size mentioned above. This appearance of apatite Bragg's reflections at 6 hours is consistent with presence of characteristic apatitic features in FTIR spectra of this glass at the same time point (Figure 2b). At 9 hours, additional reflections become visible, and clearly pronounced peaks indicate presence of apatite, and the position of the amorphous halo has shifted compared to the unreacted glass, due to formation of an ion-depleted glass. This shift in the position of the amorphous halo is also visible for the low phosphate content glass B (Figure 2c). At later time points, peaks become even more pronounced. Lines are still very broad indicating small size and highly disordered character of the crystals.

Figure 3d shows that at one week all high phosphate content glasses (A2 to H2) clearly show presence of apatite by XRD. By contrast, for the low phosphate content glasses (Figure 3c) peaks of fluorite (CaF_2, JCPD 35-816) at 28, 47 and 56°2θ dominate the XRD pattern for increasing fluoride content. The high phosphate content glasses show presence of very small amounts of fluorite (Figure 3d) with increasing fluoride content in the glass. Glass B2 (Figure 2d) shows a small peak at 56°2θ, which could suggest presence of small amounts of fluorite in that composition. Fluorite, rather

than FAp, forms when the amount of phosphate present relative to those of calcium and fluoride is not sufficient for apatite formation.
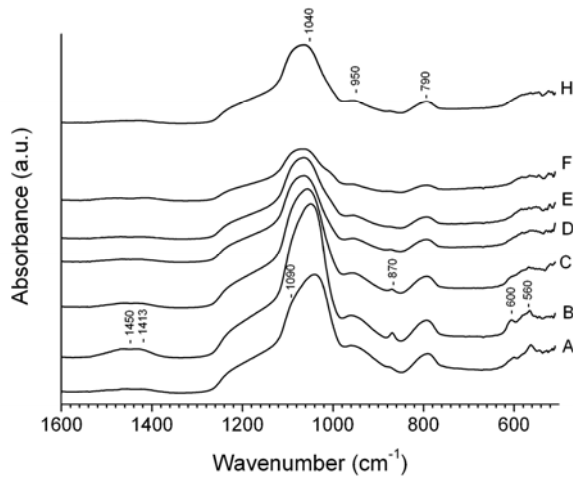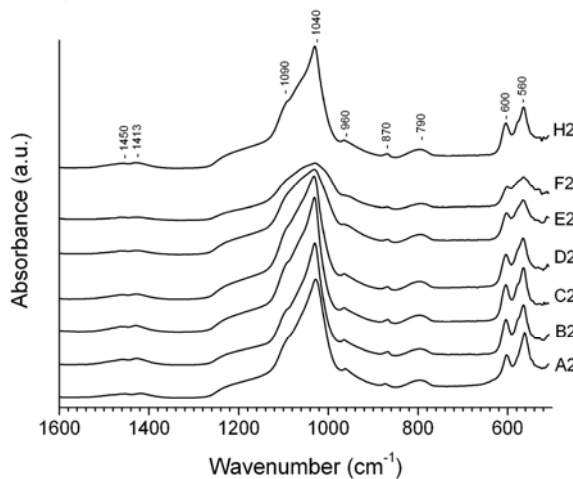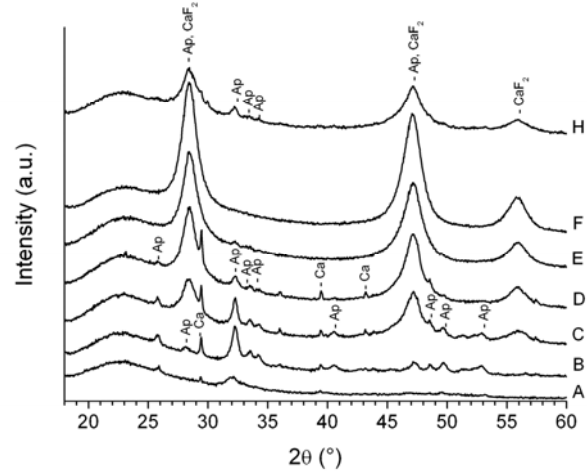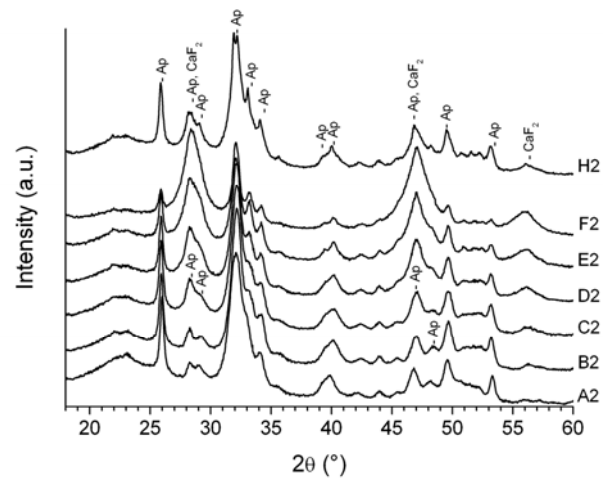

Figure 3: FTIR spectra (a, b) and XRD patterns (c, d) of low (top) and high (bottom) phosphate content glass powders at 1 week immersion in tris buffer.

Both FTIR and XRD results for the low phosphate content glasses (Figures 2c and 3c) suggest that presence of small amounts of fluoride favours apatite formation (as seen by comparing peak intensities for glasses A and B). These results are in contrast to our previous study in SBF, where glass B lacked the typical apatitic features in FTIR and XRD, resulting in our conclusion that presence of small amounts of fluoride inhibited apatite formation [4]. As fluorapatite shows a much lower solubility compared to HAp or HCA, one would expect small fluoride concentrations to favour apatite deposition, and our results in this study confirm this. The reasons for the previous poorer performance of glass B cannot be fully explained at this stage; however, variation in the amounts or particle sizes of powders used in the XRD study might affect the intensity of the pattern.

Our results show that the formation of apatite occurred more rapidly as the phosphate content increased (Figures 2c and d), although the network connectivity (NC) was kept constant, which indicates that in these glasses the phosphate content is a more important variable than NC (or possibly an overriding factor in a process where NC and phosphate dissolution compete).

Supplementary Figure S3a shows XRD patterns of glasses C2 and H2 (which is a sodium-free version of glass C2) at 1 week immersion in tris buffer. While peak intensities are comparable for both compositions, glass H2 shows more clearly pronounced and better resolved peaks: glass C2 shows only a single broad at $32.2°2\theta$ only; glass H2 shows the two peaks at 31.8 and $32.2°2\theta$ (JCPDS 09-432) to be clearly resolved (Figure S3b), indicating a higher degree of crystallinity. In addition, glass H2 clearly shows apatite peaks at 6 hours in tris buffer (Figure S3c), while glass C2 shows a distorted amorphous halo only at this time point, suggesting presence of very small amounts of apatite only. This suggests that the all calcium glass forms apatite significantly faster than the sodium-containing composition, and also forms a more crystalline apatite. One reason for this could be the higher calcium content in glass H2 compared to C2, resulting in an increased release of calcium ions and subsequently increased apatite formation. A similar effect was observed for the low phosphate content glasses in SBF [4]. While the sodium-containing glass C2 would be expected to have a higher solubility (due to Na^+ ions providing a less efficient cross-linking of the silicate chains compared to Ca^{2+} ions, as described previously [4,5]), our results might suggest that the increase in calcium content increases apatite formation despite reduced solubility. However, according to Figures 3a and c, when tested in tris buffer, sodium-free low phosphate content glass H does not show increased apatite formation compared to glass C. An alternative explanation for the increased apatite formation of glass H2 compared to C2 is the presence of small amounts of apatite in glass H2 before the glass was treated in tris buffer (Supplementary Figure S1). Usually nucleation is the limiting factor in crystallisation processes, and these apatite crystals already present in the glass, although low in concentration, could favour apatite formation compared to a glass which is free of apatite crystals.

A ^{19}F MAS NMR spectrum (Figure 4) of glass B2 after 1 week of immersion in tris buffer shows a clearly pronounced peak at -105 ppm and a shoulder at about -90 ppm. Low phosphate content glasses previously showed presence of a broad shoulder on the low frequency side (right hand side) of the peak between about -140 ppm to -150 ppm, due to a residual glass phase (due to mixed sodium calcium fluoride species in the glass structure [8]) or due to mixed Ca/Na fluorine complexes adsorbed on the residual glass powder. The absence of a shoulder in this range of the spectrum in Figure 4 suggests that the high phosphate content glass has degraded more compared to the low phosphate content glass, which agrees with our results of increased apatite formation in glass B2 compared to glass B (*cf.* above). While the cause of the shoulder at -90 ppm cannot be fully explained at this stage and requires detailed further investigation, the signal at -105 ppm was assigned to overlapping peaks of fluorapatite (-103 ppm) and fluorite (-108 ppm), as

described previously for low phosphate content glasses treated in SBF [4]. This suggests that the high phosphate content glasses form FAp, rather than HCA or HAp in tris buffer, similarly to the low phosphate content glasses in SBF. In addition, it shows that despite a significant increase in phosphate content in the glass we do still see formation of fluorite, which is confirmed by the presence of fluorite peaks in XRD patterns (Figures 2d and 3d). Fluorite formation can be explained by the fact that experiments were performed in a solution devoid of phosphate ions, in contrast to SBF which contains phosphate concentrations similar to those in physiological solutions. Therefore the phosphate for apatite formation in the present study has to be released from the glass powders. In physiological solutions such as saliva which contain PO_4^{3-} (albeit in varying concentrations), the glasses would be expected to perform even better, with formation of fluorite being negligible and apatite formation occurring at time points even less than 6 hours.
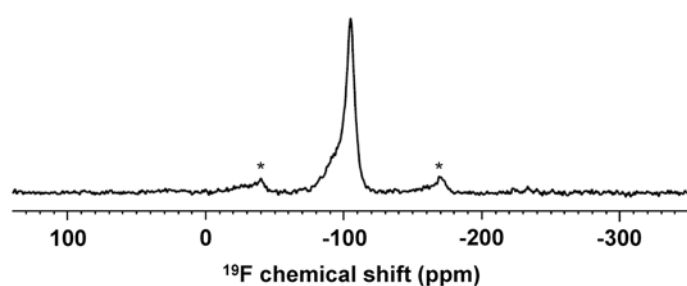

Figure 4. ^{19}F MAS-NMR spectrum of glass B2 at 1 week immersion in tris buffer. Spinning side bands are marked by an asterisk.

It is important to note that structural considerations are a prerequisite when increasing the phosphate content of bioactive glasses for improving degradation and apatite formation. As shown previously, additional network modifier cations (such as Ca^{2+} or Na^+) need to be added to charge balance the phosphate units (PO_4^{3-}) in the glass [7]. If the phosphate content is increased without additional cations for charge balancing, the silicate network becomes more cross-linked [7], resulting in a reduction in solubility, degradation and apatite formation [14]. Similarly, calcium fluoride needs to be added to the glass composition (thereby keeping the ratio of all other components constant), in order to avoid cross-linking of the silicate network [8] and in order to maintain degradation and bioactivity of the glasses [4,8].

Glass dissolution and ion release in tris buffer

For all glasses, elemental concentrations (Figure 5 for high phosphate content glasses; results for low phosphate glasses follow similar trends and are shown in Supplementary Figure S4) increase upon glass immersion, which is to be expected as the tris buffer solution is free of the elements (Ca, P, Na, Si and F) investigated in this study. The use of tris buffer is often considered of interest for studying the ion release kinetics as bioactive glasses, as apatite formation (in

contrast to studies performed in SBF) is usually not expected. However, as our glasses clearly formed (fluor)apatite in tris buffer, this has to be taken into account when discussing the ionic concentrations in solution.
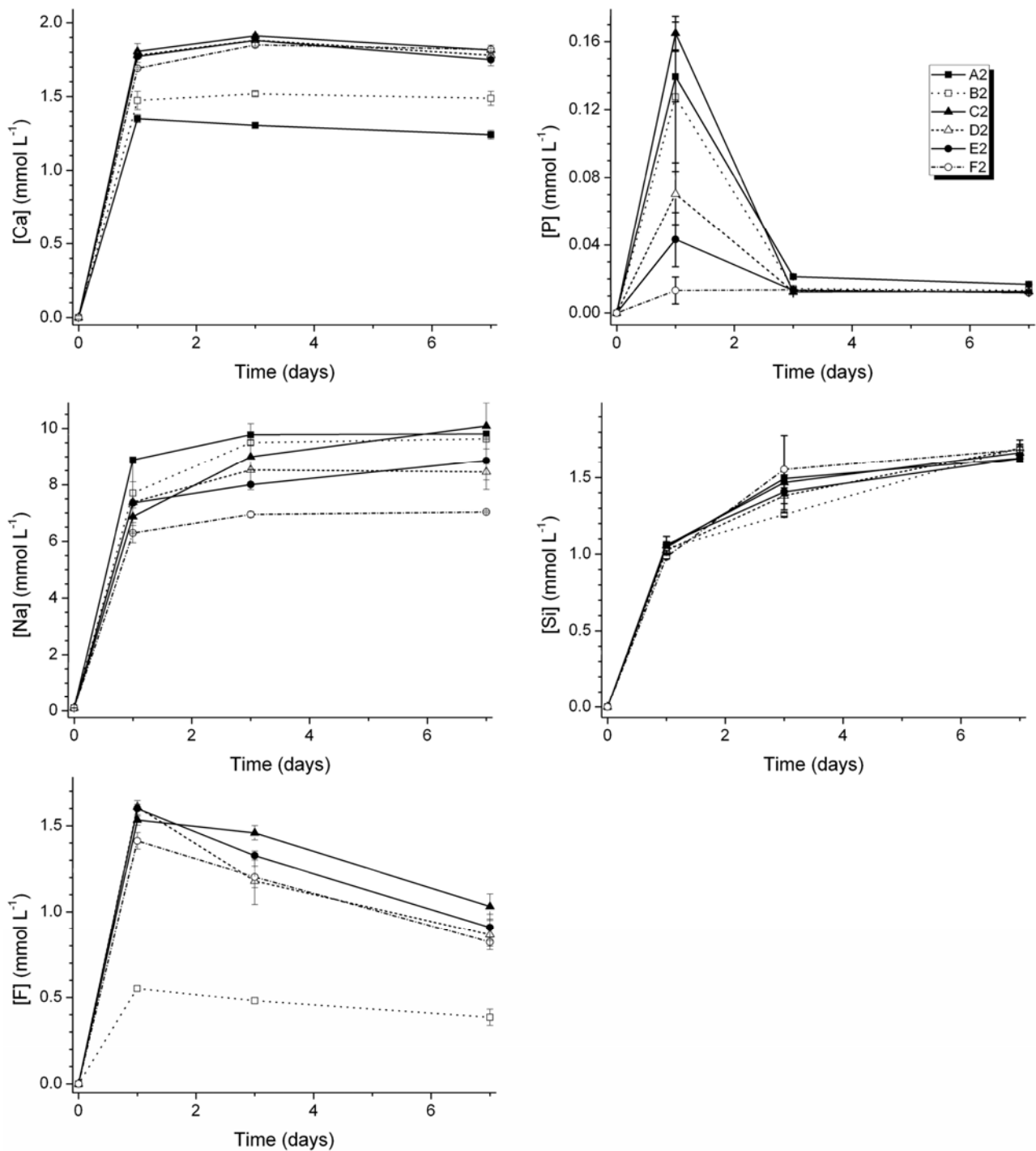

Figure 5: Elemental concentrations ± standard deviation of Ca, P, Na, Si and F in tris buffer *vs*. incubation time of high phosphate content glass powders. (Lines are drawn as a guide to the eye.)

Silicon concentrations increase continuously over the time of the experiment, *i.e.* over 7 days (Figures 5 and S4). We previously suggested that apatite forms in SBF once Si has reached the solubility limit, as formation of a silica gel layer is thought to aid nucleation of apatite [4]. However, in this study we see the presence of silica gel as a shifted

amorphous halo in XRD within 1 day for glass B and within 6 hours for glass B2. Si concentrations, however, keep

increasing after that, suggesting that the concentration of Si in solution is actually less predictive of silica gel and apatite

formation than suggested previously. This confirms results by Lusvardi *et al.* [12], which also showed that formation of

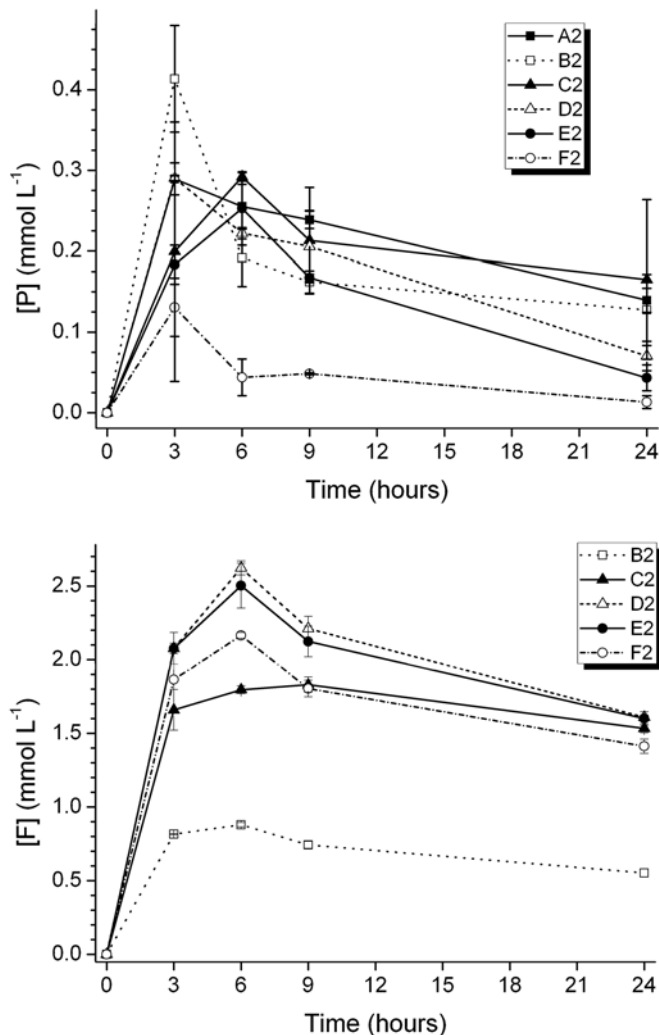a silica-gel layer is not a prerequisite for apatite formation, and that apatite therefore might precipitate from solution.

Figure 6: Elemental concentrations ± standard deviation of P and F in tris buffer *vs*. incubation time up to 24 hours of

high phosphate content glass powders. (Lines are drawn as a guide to the eye.)

Concentrations of Ca, Na and F remain relatively constant after 1 day, while the phosphate concentration drops sharply,

confirming our conclusions that the phosphate concentration is critical for apatite formation. Once all the phosphate

ions present have been consumed for apatite formation, the concentrations of calcium (between 2 and 3 mmol L^{-1} and

1.3 and 2 mmol L^{-1} for the low and high phosphate content glasses, respectively) and fluoride (between 1 and

1.7 mmol L^{-1} for all glasses) are still high, resulting in formation of fluorite. The fluoride concentrations of the high

phosphate content glasses (B2 to F2; results for H2 not shown; Figure 5) decrease slightly over time. Although the

phosphate concentrations at this time point are already low, the further release of small amounts of phosphate from the glass and the immediate formation of fluorapatite with available fluoride ions cannot be excluded.

Figure 6 shows that for the high phosphate content glasses the calcium and fluoride concentrations reach their maximum within 3 and 6 hours, after which the concentrations decrease. This is due to the fluorapatite formation at very early time points (*i.e.* within 6 hours).

Conclusions

Fluoride containing bioactive glasses form fluorapatite in tris buffer solution, which is more acid resistant than hydroxy-carbonate apatite. Apatite formation occurred more rapidly (within 6 hours) with increased phosphate content in the glass compared to 3 days for low phosphate content glasses. An increase in phosphate content in the glass also favoured formation of fluorapatite rather than fluorite, and allowed for apatite formation at lower pH, which is favourable for applications in both dentistry and orthopaedics. High phosphate content fluoride-containing glasses are particularly suited for use in remineralising dentifrices for treating dentine hypersensitivity, as the phosphate ions present in saliva should result in apatite formation within even less than 6 hours, *i.e.* well within a typical overnight sleep period of 8 hours. But also for other applications such as bone fillers, scaffolds for tissue engineering or coatings of metallic implants, the design of high phosphate content glasses which are highly bioactive is of great interest. Our results show that the bioactivity of glasses can be increased significantly, if glasses are designed based on a good understanding of their structure-property relationship.
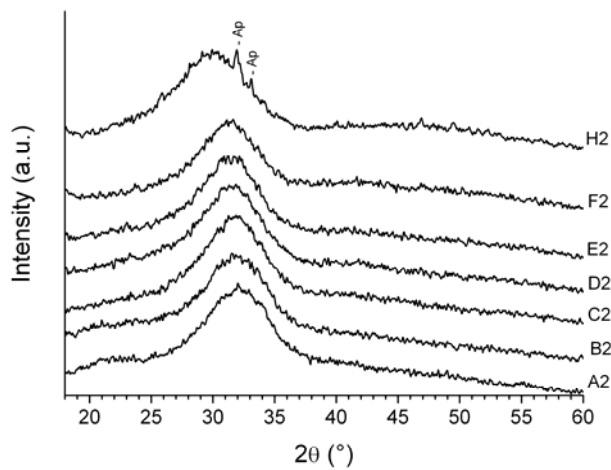
Acknowledgements

Appendix A: Supplementary data

Figure S1: XRD patterns of powders of high phosphate content glasses; peaks are apatite (Ap). (The dotted line is
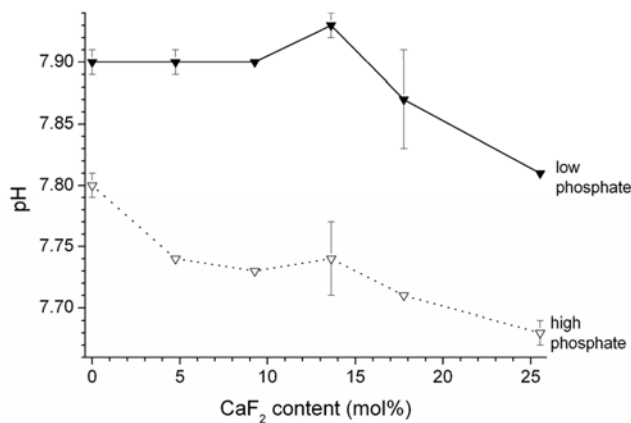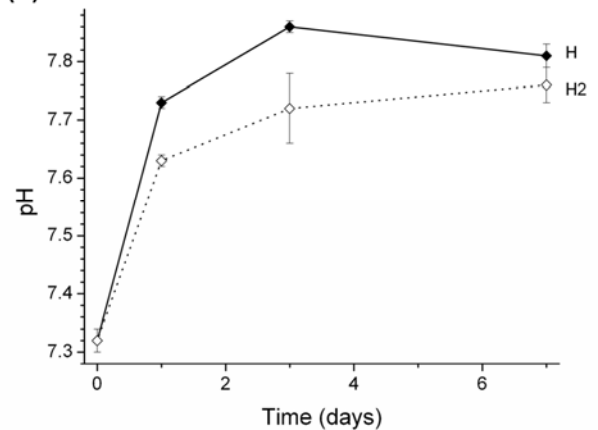
drawn as a guide to the eye only.)

Figure S2: pH of tris buffer solution after immersion of (a) low and high phosphate content glasses for 3 days *vs.* CaF_2

content in the glass and (b) glasses H (low phosphate content) and H2 (high phosphate content) *vs.* time.

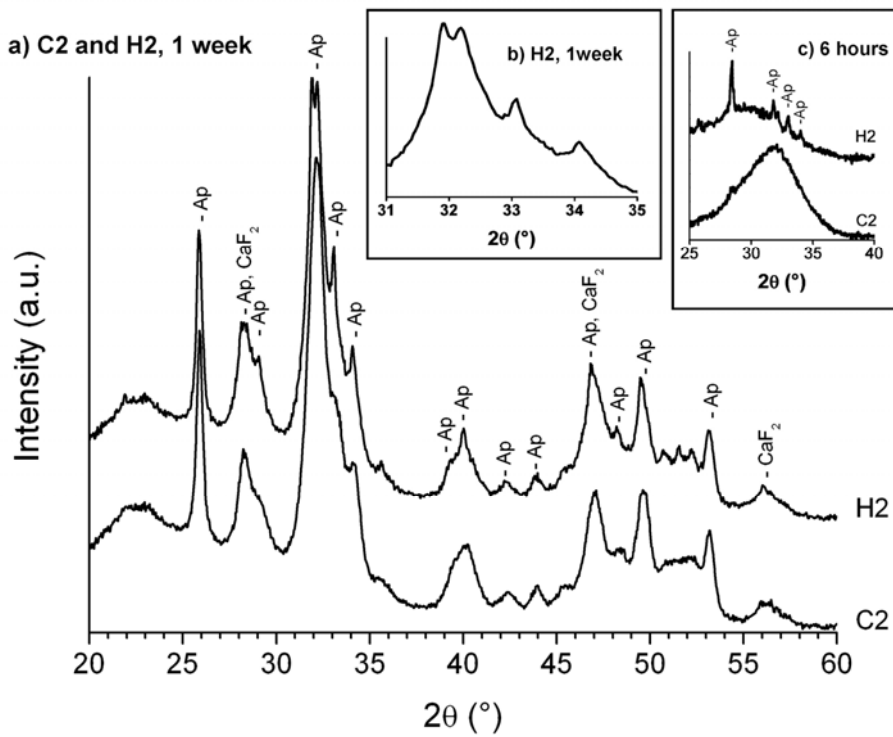(Lines are drawn as a guide to the eye only.)

Figure S3: XRD patterns of (a) glasses C2 (Na-containing) and H2 (Na-free) and (b) glass H2; both at 1 week immersion in tris buffer and (c) both glasses at six hours in tris buffer ; peaks are apatite (Ap), calcite (Ca) and fluorite (CaF_2).
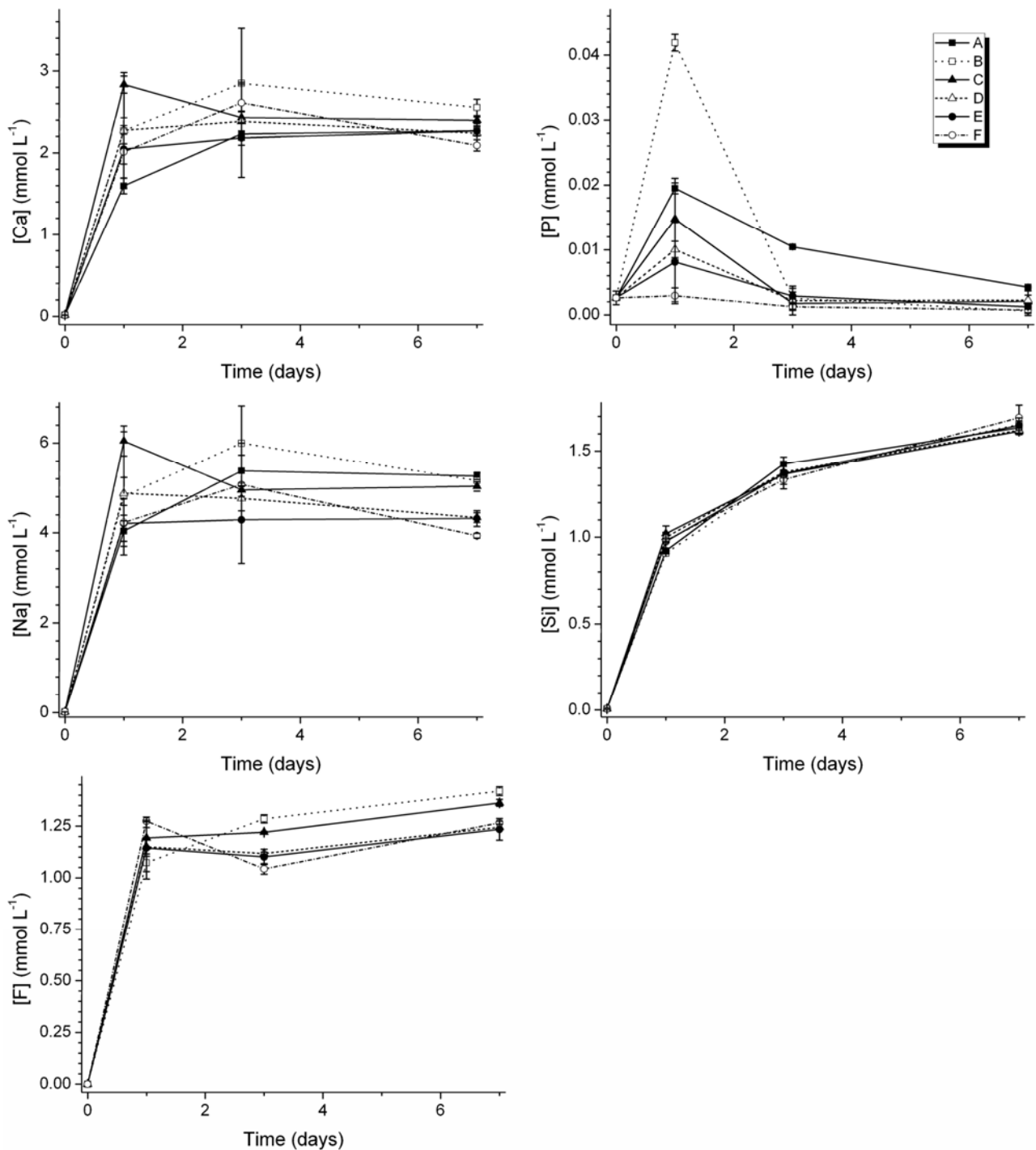
Figure S4: Elemental concentrations ± standard deviation of Ca, P, Na, Si and F in tris buffer *vs*. incubation time of low

phosphate content glass powders. (Lines are drawn as a guide to the eye.)

References

[1]   Hench LL, Paschall HA. Direct chemical bond of bioactive glass-ceramic materials to bone and muscle. J Biomed Mater Res 1973;7:25-42.

[2]   Tai BJ, Bian Z, Jiang H, Greenspan DC, Zhong J, Clark AE, et al. Anti-gingivitis effect of a dentifrice containing bioactive glass (NovaMin®) particulate. J Clin Periodontol 2006;33:86-91.

[3]   Du MQ, Bian Z, Jiang H, Greenspan DC, Burwell AK, Zhong JP, et al. Clinical evaluation of a dentifrice containing calcium sodium phosphosilicate (NovaMin) for the treatment of dentin hypersensitivity. Am J Dent 2008;21:210-4.

[4]   Brauer DS, Karpukhina N, O'Donnell MD, Law RV, Hill RG. Fluoride-containing bioactive glasses: Effect of glass design and structure on degradation, pH and apatite formation in simulated body fluid. Acta Biomater 2010;6:3275-82.

[5]   Elgayar I, Aliev AE, Boccaccini AR, Hill RG. Structural analysis of bioactive glasses. J Non-Cryst Solids 2005;351:173-83.

[6]   Lockyer MWG, Holland D, Dupree R. NMR investigation of the structure of some bioactive and related glasses. J Non-Cryst Solids 1995;188:207-19.

[7]   O'Donnell MD, Watts SJ, Law RV, Hill RG. Effect of P_2O_5 content in two series of soda lime phosphosilicate glasses on structure and properties - Part I: NMR. J Non-Cryst Solids 2008;354:3554-60.

[8]   Brauer DS, Karpukhina N, Law RV, Hill RG. Structure of fluoride-containing bioactive glasses. J Mater Chem 2009;19:5629-36.

[9]   Lusvardi G, Malavasi G, Cortada M, Menabue L, Menziani MC, Pedone A, et al. Elucidation of the structural role of fluorine in potentially bioactive glasses by experimental and computational investigation. J Phys Chem B 2008;112:12730-9.

[10]   Hill R. An alternative view of the degradation of bioglass. J Mater Sci Lett 1996;15:1122-5.

[11]   Hench LL, Spilman DB, Hench JW, inventors; University of Florida, assignee. Fluoride-modified bioactive glass (Bioglass) and its use as implant material. US patent 4775646. 1988 Oct 4.

[12]   Lusvardi G, Malavasi G, Menabue L, Aina V, Morterra C. Fluoride-containing bioactive glasses: Surface reactivity in simulated body fluids solutions. Acta Biomater 2009;5:3548-62.

[13]   Aina V, Malavasi G, Pla AF, Munaron L, Morterra C. Zinc-containing bioactive glasses: Surface reactivity and behaviour towards endothelial cells. Acta Biomater 2009;5:1211-22.

[14]   O'Donnell MD, Watts SJ, Hill RG, Law RV. The effect of phosphate content on the bioactivity of soda-lime-phosphosilicate glasses. J Mater Sci Mater Med 2009;20:1611-8.

[15]   Kokubo T, Kushitani H, Sakka S, Kitsugi T, Yamamuro T. Solutions able to reproduce *in vivo* surface-structure changes in bioactive glass-ceramic A-W. J Biomed Mater Res 1990;24:721-34.

[16]   Kim CY, Clark AE, Hench LL. Early stages of calcium-phosphate layer formation in bioglasses. J Non-Cryst Solids 1989;113:195-202.

[17]   Jones JR, Sepulveda P, Hench LL. Dose-dependent behavior of bioactive glass dissolution. J Biomed Mater Res 2001;58:720-6.

[18]   LeGeros RZ, Trautz OR, Klein E, Legeros JP. 2 Types of carbonate substitution in apatite structure. Experientia 1969;25:5-7.

[19]   Rey C, Combes C, Drouet C, Lebugle A, Sfihi H, Barroug A. Nanocrystalline apatites in biological systems: characterisation, structure and properties. Materialwiss Werkst 2007;38:996-1002.

[20]   Lu X, Leng Y. Theoretical analysis of calcium phosphate precipitation in simulated body fluid. Biomaterials 2005;26:1097-108.